Look Angle Constrained Impact Angle Control Guidance Law for Homing Missiles with Bearings-Only Measurements

Hyeong-Geun Kim[1], Jun-Yong Lee[2], and H. Jin Kim[3]

***Abstract*—This paper presents an impact angle control guidance law that confines the missile look angle during homing in order not to exceed a seeker's field-of-view limit. A sliding surface variable whose regulation guarantees the interception of a stationary target at the desired impact angle is designed, and the guidance law is derived to make the surface variable go to the sliding mode. Using a magnitude-limited sigmoid function in the surface variable, the proposed law prohibits the look angle from exceeding the specified limit during the entire homing. This capability to confine the missile look angle is valuable when a seeker's field-of-view is restricted, since imposing the terminal impact angle constraint demands the missile to fly a curved trajectory. Furthermore, the proposed law can be implemented under bearings-only measurements because the command does not involve any information of the relative range and line-of-sight rate. Numerical simulations are conducted to demonstrate the validity of the proposed law. The result shows that the proposed guidance law accomplishes the impact angle constraint without violating the prescribed look angle limit although it only uses the information of bearing angles.**

***Index Terms*—Homing guidance, impact angle control, field-of-view limits, bearings-only measurements**

I. Introduction

Since the first attempt of imposing the terminal impact angle constraint to the guidance problem in [1], much investigation related to the impact angle control guidance (IACG) has been made [1]–[20]. Particularly, various recent research about advanced guidance laws considering IACG focuses on practical issues such as limited field-of-view (FOV) constraint or restriction of available target information.

For practical implementation of IACG, the limited FOV condition is a significant factor because the curved trajectory may let the seeker's look angle exceed the confined FOV limit. Especially when the missile is equipped with a strapdown seeker which has a narrow angle of view, this consideration is an essential task in terms of maintaining the seeker lock-on condition. In this regard, there have been several studies about IACG with consideration of the confined FOV limit, and these previous works can be classified into two categories of methods based on linearized dynamics [12]–[15] and nonlinear approaches [16]–[20].

In common linear methods, the guidance law is designed as a polynomial form of time-to-go or relative range. In [12], a guidance law made up of time-to-go polynomial is developed in order to achieve the desired impact angle with zero terminal command. With linearization of the flight path angle, the entire look angle profile of the closed-loop under the law in [12] is obtained as a polynomial form, which enables the user to modulate the maximum magnitude of missile look angle by adjusting a set of gains in advance. The guidance law in [13] is formulated as a sum of the time-to-go polynomial guidance command of [12] and an additional term proportional to the cross range. In this way, the homing missile moves with an oscillatory trajectory normal to the desired collision course, which allows the target observability to be enhanced compared with the conventional time-to-go polynomial guidance. Like the work in [12], adjusting the polynomial gains beforehand also enables to confine the maximum missile look angle [13].

Unlike the laws in [12] and [13] explained above, which precalculate the maximum magnitude of the look angle based on the closed-loop trajectory solution, the guidance law in [14] directly handles the look angle constraint during the homing phase by adopting the optimal control theory. A general optimal control problem that involves an inequality constraint of the state variable is investigated in [21]. The authors in [14] apply an optimal control problem to the missile engagement dynamics in order to limit the missile look angle by the inequality constraint. Consequently, the law in [14] can prevent the look angle from exceeding the prescribed value. As an advanced version of the work in [14], a range-to-go weighted optimal guidance law is developed in [15]. Similar to [14], the optimal control theory is applied with the state variable inequality constraint in order to fulfill the IACG without violating the FOV limit. The range-to-go is additionally multiplied in the performance index of the control energy, so the terminal command converges to zero unlike the law in [14].

The laws in [12]–[15] mentioned above, derived based on the linearized engagement kinematics, require the knowledge of the relative range between the missile and target because all these laws are expressed as functions of time-to-go or range-to-go. When the missile system is equipped with a passive sensor such as an infrared seeker or a passive sonar, however, the range information is difficult to measure in real time. In this regard, several nonlinear guidance laws

[1]Hyeong-Geun Kim is a Doctoral Student in the Department of Mechanical and Aerospace Engineering, Seoul National University, Seoul, South Korea; lwmhg@snu.ac.kr

[2]Jun-Yong Lee is a Doctoral Student in the Department of Mechanical and Aerospace Engineering, Seoul National University, Seoul, South Korea; jylee1215@snu.ac.kr

[3]H. Jin kim is a professor in the Department of Mechanical and Aerospace Engineering, Seoul National University, Seoul, South Korea; hjinkim@snu.ac.kr

utilizing the characteristics of the pure proportional navigation (PPN) guidance or biased pure proportional navigation (BPPN) guidance which does not require the accurate measurement of the relative range have been proposed.

Because the conventional PPN guidance does not fulfill the impact angle control, multi-phase composite guidance schemes which switch the navigation constants or biased terms during homing are adopted for achieving the IACG in several studies [10], [11], [16]–[20]. Although the look angle limitation is not considered, the studies in [10] and [11] are valuable that take advantage of the IACG using the switched-gain based guidance. Using the properties that the PPN guidance with the navigation constant of $N < 2$ can achieve any terminal impact angle and PPN with $N = 2$ accomplishes the interception of the stationary target without command convergence, the two-phase PPN guidance law in [10] can fulfill the IACG in surface-to-surface engagements. As an extension for the case against a non-stationary and non-maneuvering target, a similar composite PPN guidance law is also developed in [11].

Based on this multi-phase guidance structure, several IACG laws involving the FOV constraint are addressed. The authors in [16] propose a two-phase guidance scheme composed of the PPN guidance and BPPN guidance. Since the closed-loop solution under the two-phase law is obtained in this paper, the desired duties such as satisfying the terminal impact angle without violating the look angle limitation can be achieved by adjusting the integral of the bias profile. However, because a specific condition for limiting the look angle is not given analytically in this work, a selection of the bias profile is proceeded by trial and error in order not to violate the limited FOV condition. As an improved version of the law in [16], two types of laws, i.e. switched-gain PPN (SGPPN) and switched-bias PPN (SBPPN), are designed in [17]. These two laws provide specified conditions that guarantee the satisfaction of the look angle constraint, so the desired tasks can be achieved more readily compared with the law in [16]. The work in [18] proposes a look angle constrained guidance law that considers the limited acceleration constraint. Similar to the works in [16] and [17], the navigation gains for satisfying the desired constraints are calculated by numerical solving. By the fact that the PPN with $N = 1$ maintains the look angle as a constant, the switched-gain PPN law in [19] satisfies the constraints on the impact angle and look angle with a navigation constant changing from $N = 1$ to $N = N_s \geq 2$. The study in [20] deals with not only the look angle constraint but also the acceleration command limitation by developing a BPPN guidance law that switches the bias term. The designed BPPN law with the navigation constant of $N > 2$ also achieves zero terminal command because the bias term converges to zero at the terminal stage.

The above composite guidance laws in [16], [17], [19], [20] except for [18] do not involve the range information in their command. Although the law in [18] requires the knowledge of relative range for embodying the switching scheme, the measurement of the range is not necessary for its implementation because an observer estimating the range is also developed with the guidance law. Therefore, the laws in [16]–[20] are useful when the guided system is equipped with a passive sensor or jammed by an electronic attack such as an electronic countermeasure (ECM) because the range information is not required.

In this study, we propose an impact angle control guidance law that restricts the seeker look angle within the prescribed limits. To develop the guidance law, error variables that aim to satisfy the interception and impact angle constraints are defined, and the guidance command is derived by letting the defined variables converge to zero based on the sliding mode control technique. In the control structure, the magnitude of the look angle is restricted by using a magnitude-limited sigmoid function. The effectiveness of utilizing the sigmoid function to satisfy the seeker's FOV constraint is demonstrated in the previous works [22] and [23] where *impact time* control guidance laws considering the seeker's FOV constraint are presented. Such property also applies to the law proposed in this paper, allowing interception of a stationary target at the desired *impact angle* without violating the prescribed FOV limits as will be explained below.

Compared with the previously published studies related to IACG with considering the limited FOV constraint in [12]–[20], the proposed work in this study has the following contributions. First, the developed law does not demand any knowledge of the time-to-go or relative range unlike the existing linear methods in [12]–[15]. Therefore, the proposed law can easily be implemented onto a missile equipped with a passive seeker.

Another advantage is that the proposed law does not involve the LOS rate information unlike the existing PPN-based nonlinear methods in [16]–[20]. That is, just bearings-only measurement without estimating the relative range or LOS rate is enough for the implementation of the proposed guidance law, so it provides advantages of jamming avoidance and low development cost by allowing a structurally simple sensor such as a strapdown passive seeker.

In addition, the application of the proposed law does not require numerical computation during the entire homing unlike several laws in recent studies [14], [15], [17], [18]. Thus, an issue of performance reduction caused by lack of calculation time or capacity needs not be considered when employing the guidance law.

The remainder of this paper is organized as follows: In section II, the formulation for the impact angle control problem is described. In section III, the guidance law is derived based on the sliding mode control technique. Sections IV and V substantiate the validity of the proposed law by theoretically analyzing the closed-loop dynamics and carrying out numerical simulations respectively. The contribution and summary of this paper are remarked in section VI.

II. Problem Statement

This section gives the nonlinear dynamics of the planar engagement against a stationary target to formulate the guidance problem for impact angle control. Figure 1 illustrates the two-dimensional geometry for the engagement between the missile and target denoted as M and T respectively. The frame $X_I O_I Y_I$ represents the inertial coordinate, and V_M, γ_M and

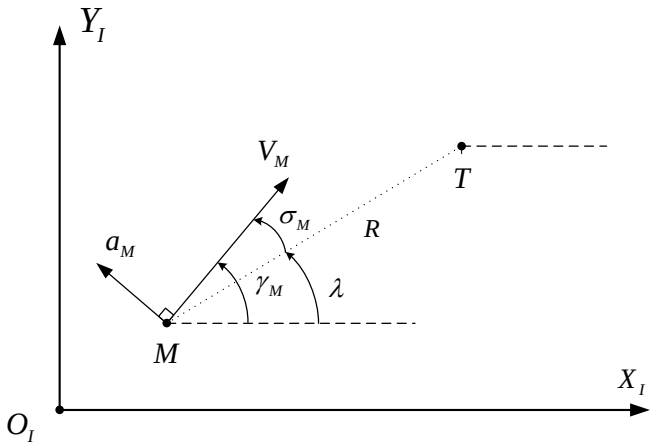

Fig. 1: Two-dimensional engagement geometry against a stationary ground target

a_M denote the speed, flight path angle and normal acceleration of the missile respectively. σ_M is the look angle defined as the angle between the LOS and missile heading under the assumption that the angle of attack is small enough to be neglected. The straight line between the missile M and target T is referred as the line-of-sight (LOS). R mean the relative range along the LOS and λ represent the included angle between the LOS and ground axis. Based on the variables defined in Fig. 1, we express the governing equations as

$$\dot{R} = V_R \tag{1a}$$

$$R\dot{\lambda} = V_\lambda \tag{1b}$$

where V_R and V_λ represent the relative velocity component of the target to the missile along and perpendicular to the LOS respectively as

$$V_R = -V_M \cos\sigma_M \tag{2a}$$

$$V_\lambda = -V_M \sin\sigma_M \tag{2b}$$

where the missile speed V_M is assumed to be constant in our problem. Since the normal acceleration a_M is applied to the missile velocity vector, the equation of the flight path angle is written as

$$\dot{\gamma}_M = \frac{a_M}{V_M} \tag{3}$$

Our design objective of the guidance law is to intercept the target with the desired impact angle without violating the prescribed look angle limits, which is expressed mathematically as

$$R(t_f) = R_f \tag{4a}$$

$$\gamma_M(t_f) = \gamma_d \tag{4b}$$

$$|\sigma_M(t)| \le \sigma_M^{\max} \le \pi/2 \quad \forall t \in [0, t_f] \tag{4c}$$

where t_f, R_f, γ_d and $\sigma_M^{\max}$ are the final time, acceptable maximum miss distance, desired impact angle and prescribed look angle limit. Furthermore, we assume the bearings-only measurement of the missile. Therefore, the guidance law is designed to achieve the constraints in (4) using only the LOS angle and look angle without involving the LOS rate and relative range.

III. Design of impact angle control guidance law

This section introduces the kinematic conditions for achieving the impact angle control without violating the FOV constraint during the homing, and presents a sliding mode-based guidance law to satisfy the formulated conditions.

A. Kinematic conditions for impact angle control guidance

The collision path on which the missile moves toward the target along the LOS is achieved by nullifying the missile look angle as

$$\sigma_M = 0 \tag{5}$$

In addition, choosing the collision path whose direction is equal to the desired impact angle guarantees the satisfaction of impact angle constraint, which is equivalent to

$$\lambda = \gamma_d. \tag{6}$$

Therefore, fulfilling the both conditions (5) and (6) always ensures the interception at the desired impact angle, so we define the following surface variable to achieve the desired tasks:

$$S(\sigma_M, \lambda) = e_2 - k_1 \mathrm{sgmf}(e_1, \phi_1) \tag{7}$$

where the variables e_1 and e_2 are introduced to satisfy the conditions in (5) and (6) as

$$e_1 = \lambda - \gamma_d \tag{8a}$$

$$e_2 = \sigma_M, \tag{8b}$$

and the sigmoid function $\mathrm{sgmf}(\cdot)$ is defined as

$$\mathrm{sgmf}(x, \phi) = \frac{x}{\sqrt{x^2 + \phi^2}} \tag{9}$$

The user chosen parameters k_1 and ϕ_1 are constants such that

$$0 < k_1 < \sigma_M^{\max} < \frac{\pi}{2}$$

$$0 < \phi_1. \tag{10}$$

Then, the regulation of the S defined in (7) yields

$$\begin{aligned} \frac{d}{dt}\left(\frac{1}{2}e_1^2\right)\Big|_{S=0} &= e_1\dot{\lambda}\Big|_{S=0} \\ &= -\frac{V_M}{R} e_1 \sin\{k_1 \mathrm{sgmf}(e_1, \phi_1)\} \\ &< 0 \quad \forall e_1 \in \mathbb{R} - \{0\} \end{aligned} \tag{11}$$

where the inequality (11) is obtained by the fact that $0 < k_1 \le \pi/2$ from (10). Thus, the variable e_1 approaches zero, which also enables $e_2 \to 0$ from (7). Here, to guarantee the achievement of the desired conditions (5) and (6) indisputably, it should be additionally verified that e_1 goes to zero before homing is over. The analysis about this issue of finite time convergence is dealt with in section IV-C.

Also note that the proposed surface variable S consists only of the look angle and LOS angle. It accords with the design requirement to implement under the bearings-only measurement. From now on, we denote the surface variable as $S(\sigma_M, \lambda)$ or $S(\sigma_M(t), \lambda(t))$ when the dependence on σ_M and λ needs to be emphasized. Otherwise, we denote as S

for brevity. In the next subsection, we design a sliding mode-based guidance law that stabilizes S at the origin based on the Lyapunov stability theory. The condition in (4c) is also taken into account during the design process in order to satisfy the FOV constraint.

B. Derivation of guidance law

From (1) and (3), the dynamics of S in (7) is obtained as

$$\dot{S} = \frac{a_M}{V_M} + \Delta \tag{12}$$

where the unknown term Δ composed of the LOS rate is

$$\Delta = -\left[1 + k_1 \frac{\partial}{\partial e_1}\left\{\text{sgmf}(e_1, \phi_1)\right\}\right]\dot{\lambda} \tag{13}$$

and its magnitude is bounded as

$$\begin{aligned} |\Delta| \leq & \frac{V_M}{R_f}\left\{1 + k_1 \frac{\phi_1^2}{\left(e_1^2 + \phi_1^2\right)^{3/2}}\right\}|\sin\sigma_M| \\ \triangleq & \frac{V_M}{R_f} f_2(\sigma_M, \lambda) \end{aligned} \tag{14}$$

The term $f_2(\sigma_M, \lambda)$ represents

$$f_2(\sigma_M, \lambda) = \left\{1 + k_1 \frac{\phi_1^2}{\left(e_1^2 + \phi_1^2\right)^{3/2}}\right\}|\sin\sigma_M|. \tag{15}$$

Based on the dynamics in (12), we propose a sliding mode guidance law for the convergence of S as follows:

$$a_M = -\left\{\frac{V_M}{R_f} f_2\left(\sigma_M, \lambda\right) + k_2\right\} V_M \text{sgn}\left(S\right) \tag{16}$$

where k_2 is a positive constant and $\text{sgn}(\cdot)$ represents the signum function. In our work, the finite time convergence of S is required since the desired conditions (5) and (6) should be achieved before the interception to fulfill the impact angle control. Therefore, sliding mode control is appropriate for designing the guidance law owing to its capability to allow finite time convergence.

Note that the proposed command in (16) does not include any variable of the LOS rate or range because S and $f_2(\sigma_M, \lambda)$ in (16) are composed of only the look angle and LOS angle as shown in (7) and (15). Therefore, just bearings-only measurement is enough for the implementation of the proposed guidance law.

Now, we obtain the closed-loop dynamics of S by substituting (16) into (12) as follows:

$$\dot{S} = -\left\{\frac{V_M}{R_f} f_2\left(\sigma_M, \lambda\right) + k_2\right\} \text{sgn}(S) + \Delta. \tag{17}$$

Since achieving the sliding mode $S = 0$ enables the interception of the stationary target at the designated impact angle as shown in subsection III-A, we verify the stability of $S = 0$ using the closed-loop dynamics of (17) in next section IV.

IV. Analysis of the Proposed Law

This section substantiates that the proposed guidance law satisfies the desired constraints through three subsections. In subsection IV-A, we confirm that the look angle does not violate the prescribed FOV constraint under the proposed law. In subsection IV-B, the stability of S at the origin is analyzed based on the closed-loop dynamics to verify the performance of the proposed law. Subsection IV-C examines the finite time convergence of e_1 and e_2 to investigate whether the proposed law achieves the kinematic conditions for the impact angle control before the interception.

A. Look angle analysis

To check whether the proposed law satisfies the FOV constraint, let us analyze the dynamics of the look angle σ_M under the proposed law as follows:

Theorem 1. *Consider the guidance law in (7) and (16) with the parameter k_1 satisfying (10). Then, for all initial conditions satisfying $|\sigma_M(0)| \leq \sigma_M^{\max}$, the look angle is always bounded as*

$$|\sigma_M(t)| \leq \sigma_M^{\max} \quad \forall t \geq 0. \tag{18}$$

Proof. Consider a compact set $\mathbb{A} \triangleq \{\sigma_M : |\sigma_M| \leq \sigma_M^{\max}\}$ for the proof. Now, on $\sigma_M = \sigma_M^{\max}$, the time derivative of σ_M is rewritten as

$$\begin{aligned} \dot{\sigma}_M\Big|_{\sigma_M=\sigma_M^{\max}} = & \frac{a_M}{V_M} - \dot{\lambda}\Big|_{\sigma_M=\sigma_M^{\max}} \\ = & -\left\{\frac{V_M}{R_f} f_2(\sigma_M^{\max}, \lambda) + k_2\right\} \text{sgn}\Big(S\left(\sigma_M^{\max}, \lambda\right)\Big) \\ & + \frac{V_M \sin\sigma_M^{\max}}{R} \end{aligned} \tag{19}$$

In (19), $S(\sigma_M^{\max}, \lambda)$ is always positive because k_1 is chosen as (10). Furthermore, from (15), the term $f_2(\sigma_M^{\max}, \lambda)$ in (19) is bounded from below as

$$f_2(\sigma_M^{\max}, \lambda) > \sin\sigma_M^{\max}. \tag{20}$$

Substituting (20) into (19) yields

$$\dot{\sigma}_M\Big|_{\sigma_M=\sigma_M^{\max}} < -\left(\frac{V_M}{R_f}\sin\sigma_M^{\max} + k_2\right) + \frac{V_M \sin\sigma_M^{\max}}{R} \tag{21}$$

Applying $R \geq R_f$ to inequality in (21), we have

$$\dot{\sigma}_M\Big|_{\sigma_M=\sigma_M^{\max}} < -k_2 \tag{22}$$

Likewise, on $\sigma_M = -\sigma_M^{\max}$, we can have

$$\dot{\sigma}_M\Big|_{\sigma_M=-\sigma_M^{\max}} > k_2 \tag{23}$$

Consequently, the proposed law makes the set $|\sigma_M(t)| \leq \sigma_M^{\max}$ invariant, which proves (18). □

Theorem 1 verifies that the proposed guidance law in (16) achieves $|\sigma_M(t)| \leq \sigma_M^{\max}$ if the initial condition satisfies $|\sigma_M(0)| \leq \sigma_M^{\max}$. That is, the proposed law keeps the missile look angle within the prespecified FOV limit until the interception.

B. Stability analysis

In order to verify the performance of the proposed law, this subsection investigates the stability of the surface variable S in (7). For the investigation, the closed-loop dynamics in (17) is analyzed as follows:

Theorem 2. *Consider the dynamics of the surface variable (17). Then, the surface variable $S(\sigma_M(t), \lambda(t))$ reaches zero in a finite time t_r that is bounded as*

$$t_r \leq \frac{|S(\sigma_M(0), \lambda(0))|}{k_2} \tag{24}$$

Proof. For the proof, consider the Lyapunov candidate function as

$$V = \frac{1}{2}S^2. \tag{25}$$

From (17), the time derivative of V is obtained as

$$\dot{V} = S\left[-\left\{\frac{V_M}{R_f} f_2(\sigma_M, \lambda) + k_2\right\} \mathrm{sgn}(S) + \Delta\right] \tag{26}$$

Using (14) into (26) gives

$$\begin{aligned}\dot{V} \leq & -\left\{\frac{V_M}{R_f} f_2(\sigma_M, \lambda) + k_2\right\}|S| + \frac{V_M}{R_f} f_2(\sigma_M, \lambda)|S| \\ = & -k_2\sqrt{2V}\end{aligned} \tag{27}$$

which implies that S is bounded and origin of the closed-loop dynamics in (17) is asymptotically stable. Furthermore, from [24], integrating the inequality (27) over $[0, t]$ yields

$$V^{1/2}(t) \leq -\frac{1}{\sqrt{2}}k_2 t + V^{1/2}(0), \tag{28}$$

which implies that $V(t)$ goes to zero in a finite time t_r bounded as

$$t_r \leq \frac{\sqrt{2}V^{1/2}(0)}{k_2} = \frac{|S(\sigma_M(0), \lambda(0))|}{k_2}. \tag{29}$$

□

Theorem 2 shows that the sliding mode $S = 0$ is achieved in a finite time. From (7) and (11), hence, the proposed guidance law in (16) makes the errors e_1 and e_2 approach zero. However, for achieving the homing and impact angle conditions in (5) and (6) conclusively, e_1 and e_2 have to go to zero *before* the interception. Thus, in the next subsection, we analyze the finite time convergence of e_1 and e_2 to prove the validity of the proposed guidance law.

C. Convergence analysis of error variables e_1 and e_2

From **Theorem 2** in section IV-B, we can deduce that the convergence speed of S can be made faster by increasing the user-chosen parameter k_2. Furthermore, as shown in (11), we have already proven that e_1 and e_2 converge to zero after $S = 0$ is achieved. However, unlike S whose convergence speed can be made arbitrarily faster, the convergence speed of e_1 is limited since the magnitude of the parameter k_1, related to the convergence of e_1, is restricted as shown in (10). Thus, it is necessary to verify that e_1 and e_2 go to zero before the end of the homing in order to guarantee the success of the desired tasks.

This subsection investigates the dynamics of e_1 to prove the finite time convergence of e_1 and e_2 under $S = 0$. For the convergence analysis, the following lemma is obtained priorly.

Lemma 1. *Let $f : [-1, 1] \to \mathbb{R}$ be a function such that*

$$f(x) = \sin(kx) \tag{30}$$

where the constant k is chosen as $0 < k \leq \frac{\pi}{2}$. Then, the function f satisfies

$$\begin{cases} f(x) \geq xf(1) & \text{if } x \in [0, 1] \quad (31a) \\ f(x) \leq xf(1) & \text{if } x \in [-1, 0] \quad (31b) \end{cases}$$

Proof. We prove the case $f(x) \geq xf(1)$ because the other case can be proved by the same way. In the domain $x \in [0, 1]$, f is a concave function since the second derivative of f is given by

$$\frac{d^2 f}{dx^2}(x) = -k^2 \sin(kx) \leq 0. \tag{32}$$

Therefore, from the definition of the concave function, we have

$$f((1-t)x_1 + tx_2) \geq (1-t)f(x_1) + tf(x_2) \tag{33}$$

for any x_1, x_2 and $t \in [0, 1]$. Substituting 0 and 1 into x_1 and x_2 in (33) respectively yields

$$f(t) \geq tf(1), \tag{34}$$

which accords with the inequality property in (31a). □

Now, for the convergence analysis of e_1 and e_2, we present the following **Theorem 3**.

Theorem 3. *After the sliding mode $S = 0$ is achieved, the variables e_1 and e_2 in (8a) and (8b) converge to zero as the distance between the missile and target R goes to zero.*

Proof. For the proof, we introduce the following Lyapunov candidate function:

$$V_1 = \frac{1}{2}e_1^2. \tag{35}$$

First, we prove the boundedness of e_1. On $S = 0$, the time derivative of V_1 is given by

$$\begin{aligned}\dot{V}_1\Big|_{S=0} = & -\frac{V_M \sin\sigma_M}{R} e_1\Big|_{S=0} \\ = & -\frac{V_M}{R}\sin\{k_1 \mathrm{sgmf}(e_1, \phi_1)\} e_1 \\ = & -\frac{V_M}{R}\sin\left\{k_1 \frac{e_1}{\sqrt{e_1^2 + \phi_1^2}}\right\} e_1 \\ \leq & 0.\end{aligned} \tag{36}$$

where the condition of k_1 in (10) is used. The result in (36) signifies that e_1 is bounded after S converges, so there exists a positive constant $e_1^{\max}$ such that $|e_1(t)|_{S=0} \leq e_1^{\max}$. Then, from (36), we obtain

$$\dot{V}_1\Big|_{S=0} \leq -\frac{V_M}{R}\sin\left\{k_1 \frac{e_1}{\sqrt{(e_1^{\max})^2 + \phi_1^2}}\right\} e_1. \tag{37}$$

In (37), the relative range R satisfies $R \leq V_M t_{go} = V_M(t_f - t)$ where t_{go} and t_f denote the remaining time-to-go and impact time of the missile respectively, since R is the shortest distance between the missile and target. Furthermore, by **Lemma 1**, the sine term in (37) satisfies

$$\begin{cases} \sin\left\{k_1 \dfrac{e_1}{\sqrt{(e_1^{\max})^2+\phi_1^2}}\right\} \geq (\sin k_1)\dfrac{e_1}{\sqrt{(e_1^{\max})^2+\phi_1^2}} \\ \text{if } e_1 \geq 0 \end{cases} \tag{38a}$$

$$\begin{cases} \sin\left\{k_1 \dfrac{e_1}{\sqrt{(e_1^{\max})^2+\phi_1^2}}\right\} \leq (\sin k_1)\dfrac{e_1}{\sqrt{(e_1^{\max})^2+\phi_1^2}} \\ \text{if } e_1 \leq 0 \end{cases} \tag{38b}$$

Accordingly, using these properties, we have

$$\begin{aligned} \dot{V}_1\Big|_{S=0} &\leq -\frac{\sin k_1}{t_{go}} \frac{e_1^2}{\sqrt{(e_1^{\max})^2+\phi_1^2}} \\ &\leq -\frac{2\sin k_1}{\sqrt{(e_1^{\max})^2+\phi_1^2}} \frac{V_1}{t_{go}}, \end{aligned} \tag{39}$$

which implies

$$V_1(t)\Big|_{S=0} \leq V_1(0)\left(\frac{t_{go}}{t_f}\right)^{\frac{2\sin k_1}{\sqrt{(e_1^{\max})^2+\phi_1^2}}}. \tag{40}$$

The inequality in (40) implies that $V_1(t)$ goes to zero as t approaches t_f, which also yields $\lim_{t\to t_f} e_2 = 0$ because $e_2 = k_1 \text{sgmf}(e_1, \phi_1)$ on $S = 0$. Therefore, if the regulation of S is achieved, both e_1 and e_2 converge to zero as the missile approaches the stationary target. □

Theorem 2 implies that the sliding mode can be achieved before the end of the homing by adjusting the gain k_2. **Theorem 3** indicates that achievement of the sliding mode makes e_1 and e_2 converge to zero before the end of the homing since the homing is terminated when the relative R goes to zero. Consequently, the error variable e_1 and e_2 can be made zero before the end of the homing, which verifies that the proposed guidance law in (16) can satisfy the kinematic conditions in (5) and (6) during the homing. That is, the interception with the desired impact angle can be achieved under the proposed law.

V. Simulation results

This section evaluates the performance of the proposed guidance law by carrying out numerical simulations. In subsection V-A, the validity of the proposed guidance law for various terminal impact angles and field-of-view (FOV) constraints is demonstrated. In subsection V-B, we compare the proposed guidance law with other FOV-constrained impact angle control guidance laws. In subsection V-C, the performance of the proposed law in practical applications is examined using a realistic interceptor model.

When the proposed law is applied, to avoid the chattering caused by the discontinuity, the signum function $\text{sgn}(\cdot)$ in (16) is approximated as the following continuous hyperbolic tangent function [4], [6], [25]:

$$\tanh(ax) = 2\left(\frac{1}{1+\exp^{-2ax}} - \frac{1}{2}\right) \tag{41}$$

Applying such an approximation makes the variable converge to the ideal sliding mode with slight deviation which is approximately in inverse proportion to a [26]. We used the value of a as $a = 10$.

In addition, the acceleration command of the missile is saturated within $\pm 10g$, and the homing is terminated when the relative range R is less than or equal to 0.5 m in all the scenarios. The parameters used in the proposed guidance law are listed in Table I.

TABLE I: Simulation setting

Parameters	Values
Initial position of the missile $(x_M(0), y_M(0))$	$(0, 0)$ km
Position of the stationary target $(x_T(0), y_T(0))$	$(10, 0)$ km
Initial missile look angle $\sigma_M(0)$	15 deg
Missile speed V_M	250 m/s
Missile acceleration limits $\lvert a_M\rvert^{\max}$	10 $g^\dagger$
Guidance gains	$k_1 = \sigma_M^{\max} - 0.01$ $k_2 = 10$ $R_f = 0.5$ $\phi_1 = 0.15$

† g means the gravitational acceleration, i.e., $g = 9.81$ m/s^2.

A. Performance analysis of the proposed law

For the simulations of the performance analysis, this subsection considers two scenarios. The first scenario deals with engagements for different impact angle constraints with a fixed look angle limitation of $\sigma_M^{\max} = 45°$. The second scenario considers engagements for a fixed impact angle constraint of $\gamma_d = -60°$ with various look angle limitations.

The results of the first scenario are presented as Figs. 2a∼d. In the figures, the results for the desired impact angles of $-30°$, $-60°$, $-90°$ and $-120°$ are represented by the triangular, inverted triangular, rectangular and circular patterned-lines respectively.

Under the proposed guidance law, the missile intercepts the target for all the cases as illustrated by Fig. 2a. Specifically, figure 2b shows that the proposed law achieves the sliding mode with the lateral acceleration not exceeding $\pm 10g$. Owing to using the hyperbolic tangent function in (41) instead of the discontinuous signum function in the guidance command, it is seen that the convergence of S is obtained without undesirable high-frequency chattering. Since the sliding mode is achieved, both the errors e_1 and e_2 also approach zero as shown in Fig. 2c. In particular, we can observe that e_1 and e_2 converge to zero before the interception as proven by **Theorem 3** in section IV-C. Accordingly, the upper row of figure 2d provides the result that the proposed law achieves the desired impact angle for all the cases.

The trajectories in figure 2a also show that the missile takes a longer bypass as the higher impact angle is demanded. Nevertheless, the lower row of figure 2d shows that the look angle does not violate the prescribed limit $\sigma_M^{\max} = 45°$ for all the cases under the proposed guidance law. This result accords with **Theorem 1** in section IV-A.

Figures 3a∼d provide the simulation results of the second scenario. Likewise, the results with the look angle limits of

This article has been accepted for publication in a future issue of this journal, but has not been fully edited. Content may change prior to final publication. Citation information: DOI 10.1109/TAES.2018.2843600, IEEE Transactions on Aerospace and Electronic Systems

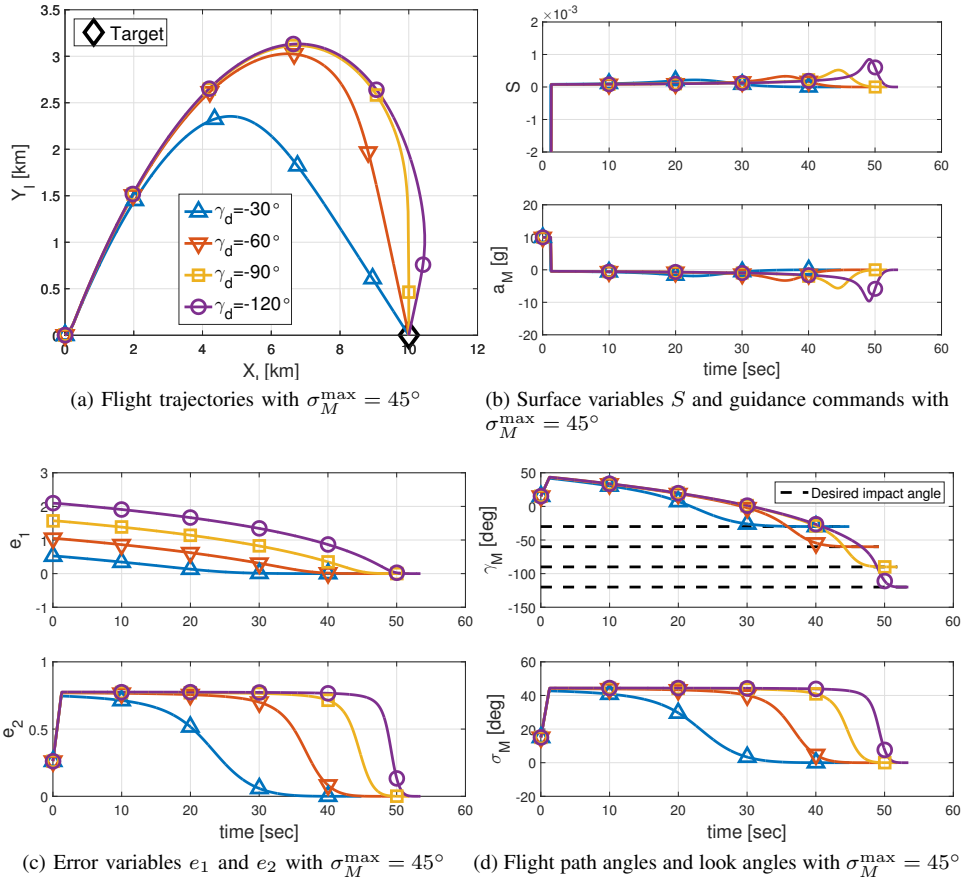

(a) Flight trajectories with $\sigma_M^{\max} = 45°$

(b) Surface variables S and guidance commands with $\sigma_M^{\max} = 45°$

(c) Error variables e_1 and e_2 with $\sigma_M^{\max} = 45°$

(d) Flight path angles and look angles with $\sigma_M^{\max} = 45°$

Fig. 2: Simulation results for different impact angle constraints with a fixed look angle limitation of $\sigma_M^{\max} = 45°$

15°, 30°, 45° and 60° are denoted as the triangle, inverted triangle, square and circle patterned-lines respectively in each figure.

Figure 3a demonstrates that the proposed law achieves the interception under all the considered FOV limits. Like the first scenario, the surface variable converges near zero at the initial stage, and then the error variables e_1 and e_2 also approach zero before the interception as shown in Figs 3b and 3c. As a result, it is observed by the upper row of Fig. 3d that the desired impact angles can be achieved for all the cases.

Figure 3a also shows that the curvatures are different from one another although the terminal impact angle is same in all the four cases. It is because all the four missiles fly under the differently prescribed values of the look angle constraints as given in the lower graph of Fig. 3d. This result demonstrates that the proposed guidance law can restrict the maximum look angle as desired, as proven in **Theorem 1**.

B. Performance comparison with other guidance laws

In this subsection, we compare the proposed law with other impact angle control guidance laws that consider the FOV limit called ROG (range-to-go weighted optimal guidance law) and TPPN (two-stage pure proportional navigation guidance law) developed in [15] and [19] respectively. ROG and TPPN are linear and nonlinear dynamics-based laws respectively, and both of them are the most recently developed laws among related research at the time of this study. These laws are generated as the following forms:

ROG [15] : (42)

$$a_M = \begin{cases} -(N+3)V_M^2\left(\frac{\sigma_M R - \sigma_M^{\max} R_1}{R^{N+3}-R_1^{N+3}}\right)R^{N+1} \\ \quad + \mu\frac{R^N}{V_M^2}\left\{1-\left(\frac{N+3}{N+2}\right)\left(\frac{R^{N+2}-R_1^{N+2}}{R^{N+3}-R_1^{N+3}}\right)\right\} \\ \qquad\qquad \text{for } R_1 < R \le R_0 \\ V_M\dot{\lambda} \\ \qquad\qquad \text{for } R_2 < R \le R_1 \\ -\frac{V_M^2}{R}\{(N+2)(N+3)\sigma_M \\ \quad + (N+1)(N+2)(\gamma_d - \gamma_M)\} \\ \qquad\qquad \text{for } R_f < R \le R_2 \end{cases}$$

TPPN [19] : (43)

$$a_M = \begin{cases} V_M\dot{\lambda} \\ N_s V_M\dot{\lambda} \end{cases} \quad \text{switches at } \lambda = \gamma_d + \frac{\sigma_M(0)}{(N_s-1)}$$

In (42) and (43), we set the parameters N and N_s as $N = 1$ and $N_s = 3$ respectively. Both settings ensure satisfaction of the impact angle and look angle constraints, and are also used in [15] and [19] respectively. Values of the other parameters such as μ, R_1 and R_2 in (42) are determined by initial conditions and the value of N.

As a simulation setting for the performance comparison, the desired impact angle is fixed as $\gamma_d = -60°$ and the FOV

This article has been accepted for publication in a future issue of this journal, but has not been fully edited. Content may change prior to final publication. Citation information: DOI 10.1109/TAES.2018.2843600, IEEE Transactions on Aerospace and Electronic Systems

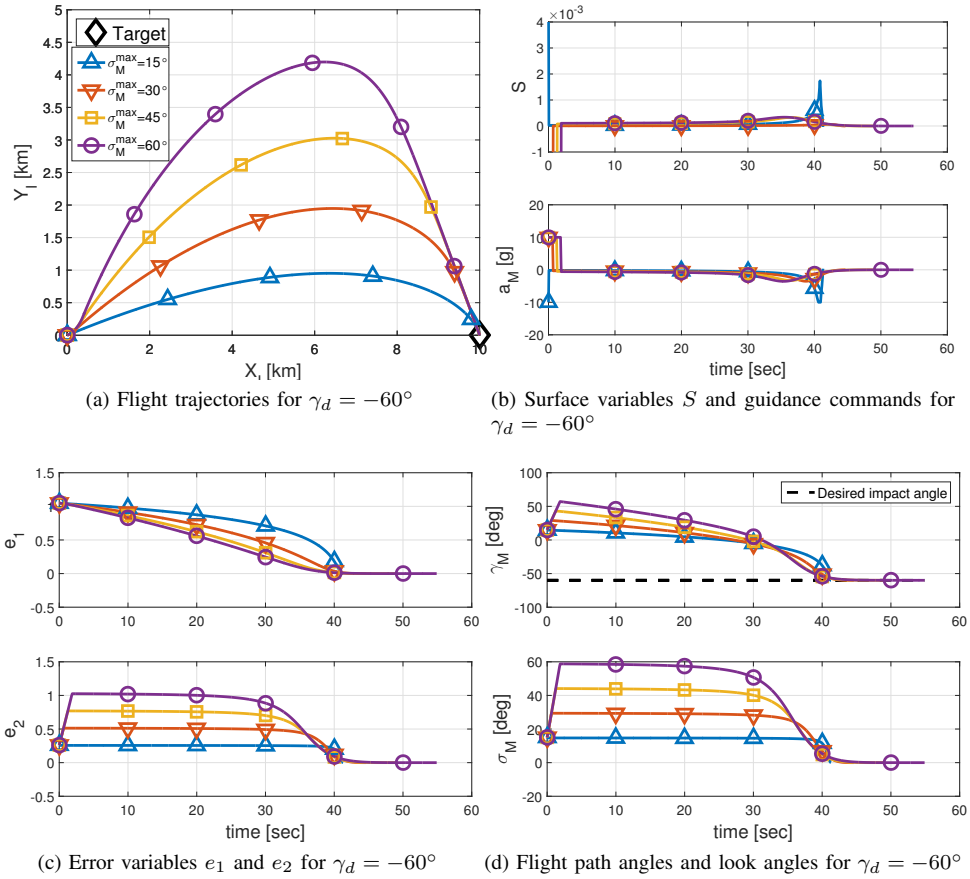

(a) Flight trajectories for $\gamma_d = -60°$

(b) Surface variables S and guidance commands for $\gamma_d = -60°$

(c) Error variables e_1 and e_2 for $\gamma_d = -60°$

(d) Flight path angles and look angles for $\gamma_d = -60°$

Fig. 3: Simulation results for a fixed impact angle constraint of $\gamma_d = -60°$ with various look angle limitations

limit of $\sigma_M^{\max} = 30°$ is applied for all three guidance laws. The initial conditions in Table I are also considered for the guidance laws except that the initial look angle for TPPN is set to be $30°$ instead of $15°$. It is because TPPN is designed so that it tries not to exceed the FOV limit by maintaining the initial look angle during the first phase as explained in detail in [19]. That is, the engagement conditions in this subsection are set to make the look angles under all the laws are constrained by the same limit, i.e. $\sigma_M^{\max} = 30°$, for fair comparison.

Figures 4a∼d give the results for an impact angle constraint of $\gamma_d = -60°$ with a look angle limitation of $\sigma_M^{\max} = 30°$ under three different guidance laws. The results under ROG, TPPN and the proposed law are denoted as the triangle, inverted triangle and circle-patterned line respectively.

Figure 4a shows that all the three guidance laws intercept the stationary target with similar trajectories. The terminal constraints on the terminal impact angle of $\gamma_d = -60°$ are also achieved without violating the look angle limit of $\sigma_M^{\max} = 30°$ under all the laws as presented by Figs. 4b and 4c.

Figure 4d provides the guidance commands under three laws. At the initial stage of the homing, TPPN generates a smaller guidance command compared with the other laws because it does not need to change the look angle as shown in Fig. 4c. This property of TPPN to maintain its initial look angle prevents the command from saturating at the initial stage. However, to achieve this property requires that the missile be launched at a deviated look angle from the target. Furthermore, since TPPN switches the navigation constant for achieving the desired impact angle, there must be an undesirable discontinuity in the guidance command as shown in Fig. 4d.

Unlike TPPN, both ROG and the proposed guidance law generate continuous commands. In particular, ROG produces the acceleration command of more modest amplitude than the other two laws except for at the initial stage, which results from its optimality property as described in detail in [15]. However, as shown in (42), the implementation of ROG needs values of transition points R_1 and R_2, which requires a numerical computation process. Hence, not enough iterations caused by lack of calculation time or capacity can result in performance degradation when employing ROG. Moreover, as shown in (16), (42) and (43), ROG necessitates the information of the relative range R while TPPN and the proposed law does not. That is, measurement or estimation of R is required for the implementation of ROG unlike TPPN and the proposed law.

In contrast, the result in Figs. 4a∼c shows that the proposed law can fulfill the impact angle control without violating the prescribed look angle limit although its implementation does not require the information of LOS rate and relative range. Figure 4d shows that the proposed law produces a large command at the initial stage to make S converge to zero, but

This article has been accepted for publication in a future issue of this journal, but has not been fully edited. Content may change prior to final publication. Citation information: DOI 10.1109/TAES.2018.2843600, IEEE Transactions on Aerospace and Electronic Systems

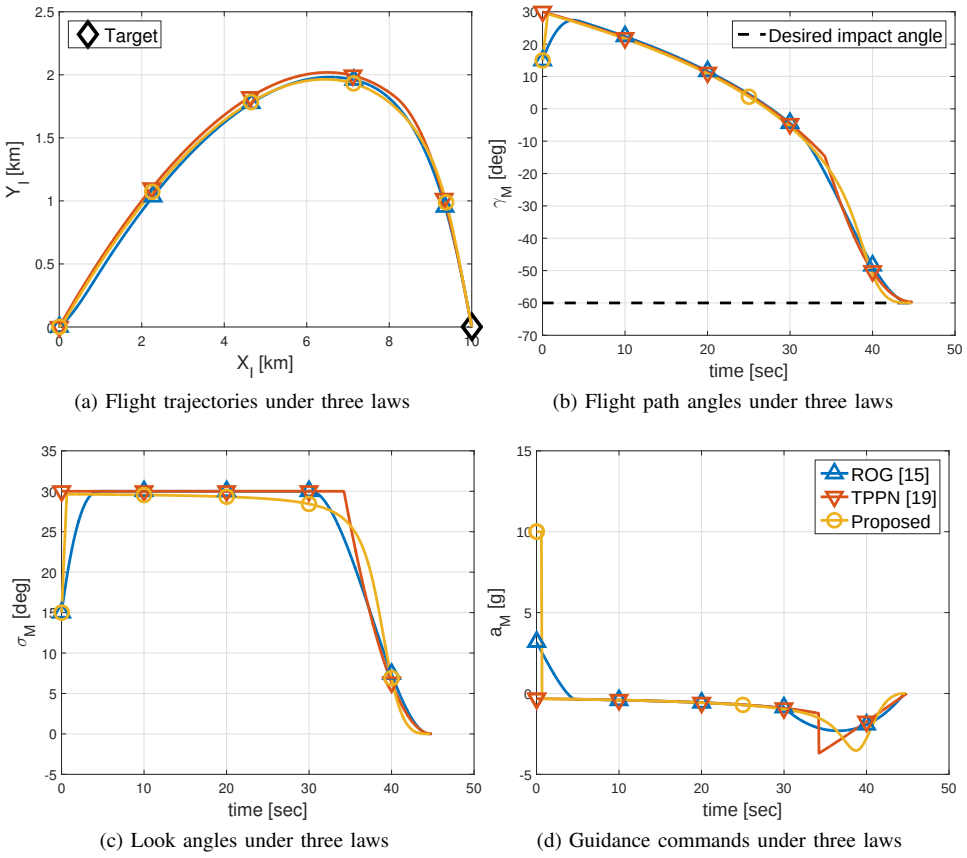

(a) Flight trajectories under three laws

(b) Flight path angles under three laws

(c) Look angles under three laws

(d) Guidance commands under three laws

Fig. 4: Simulation results under three different guidance laws: ROG in [15], TPPN in [19] and the proposed law

the generated command is continuous and not large after the initial stage. That is, the practical application of the proposed law is more helpful to restricted guidance scenarios where only bearing angles are measurable in comparison with other existing laws.

C. Performance analysis in a realistic scenario

This subsection carries out engagement simulations considering rotational dynamics of the missile to evaluate the performance of the proposed law in realistic applications. Involving the aerodynamics and gravitation, the lateral maneuvering acceleration is produced by the aerodynamic lift as

$$a_M = \frac{L(\alpha,\delta)}{m} \tag{44}$$

and the angle-of-attack α is governed by the rotational motion as

$$\begin{aligned} \dot{\alpha} =& q - \frac{L(\alpha,\delta) - mg\cos\gamma_M}{mV_M}, \quad \dot{\theta} = q \\ \dot{q} =& \frac{M(\alpha,q,\delta)}{I_{yy}}, \quad \dot{\delta} = \frac{\delta_C - \delta}{\tau_\delta}. \end{aligned} \tag{45}$$

θ, q, δ and δ_C represent the pitch angle, pitch rate, canard deflection and command of the canard deflection respectively. $L(\cdot)$ and $M(\cdot)$ mean the lift force and pitching moment, and m, I_{yy} and τ_δ denote the mass, moment of inertial with respect to the pitch axis and time constant of the canard dynamics. The detailed aerodynamic model for the lift force and pitch moment in (45) is described in [27] and [4].

Based on the realistic model, the same scenario in Fig. 2 is applied, so the desired impact angles of $-30°$, $-60°$, $-90°$ and $-120°$ with the fixed look angle limitation of $45°$ are considered. Since the angle-of-attack is not neglected in this realistic scenario, the look angle defined as the angle between the LOS and missile heading is re-expressed as

$$\begin{aligned} \sigma_M^{act} =& \theta - \lambda \\ =& \sigma_M + \alpha. \end{aligned} \tag{46}$$

In order not to violate the FOV limit, the restriction of the actual look angle in (46) is required as $|\sigma_M^{act}| \leq 45°$. To achieve the actual restriction for σ_M^{act}, σ_M in the guidance command (16) is restricted with a safety margin ε_σ, i.e., $|\sigma_M| \leq 45° - \varepsilon_\sigma$. From (46), it is reasonable that the maximum value of the angle-of-attack is selected as the safety margin. In general missile configurations, the angle-of-attack is approximately proportional to the lateral acceleration caused by the lift force as

$$\alpha \approx \frac{m}{QS_{ref}C_{L_\alpha}} a_M \tag{47}$$

where m, Q, S_{ref}, and C_{L_α} denote the mass, dynamic pressure, reference area, and coefficient of lift to angle-of-attack. Substituting $a_M = a_M^{\max} = 10g$ into (47) yields the maximum angle-of-attack, and it is calculated as $\alpha_{\max} =$

This article has been accepted for publication in a future issue of this journal, but has not been fully edited. Content may change prior to final publication. Citation information: DOI 10.1109/TAES.2018.2843600, IEEE Transactions on Aerospace and Electronic Systems

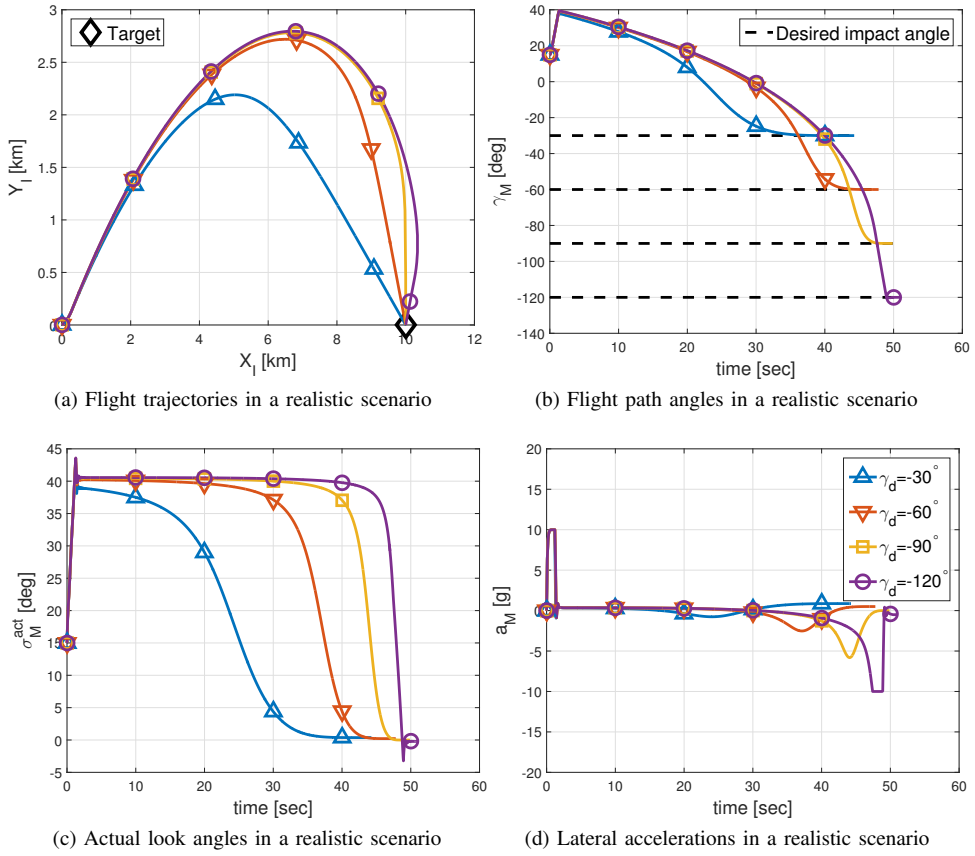

(a) Flight trajectories in a realistic scenario

(b) Flight path angles in a realistic scenario

(c) Actual look angles in a realistic scenario

(d) Lateral accelerations in a realistic scenario

Fig. 5: Simulation results in a realistic scenario

$4.425°$ in our case. Accordingly, we choose the safety margin as $\varepsilon_\sigma = 4.5°$ for this simulation in this subsection. In addition, to compensate the gravitational effect in vertical plane, the term $g\cos\gamma_M$ is added to the original command in (16).

Figure 5 presents the simulation results for the realistic scenario. The results for the desired impact angles of $\gamma_d = -30°$, $-60°$, $-90°$ and $-120°$ are denoted as the triangle, inverted triangle, square and circle patterned-lines respectively. As shown in Figs. 5a and 5b, the missile intercepts the stationary target at the desired impact angle for all cases.

From Figs. 5c and 5d, we can confirm that the proposed law satisfies the look angle limit of $\sigma_M^{act} = 45°$ with feasible lateral accelerations for all the desired impact angles. Figure 5c also shows that the actual look angle defined as (46) reaches its peak momentarily at the initial stage of the homing for every case. This large demand on the actual look angle is caused by the fact that the large requirement on the lateral acceleration at the initial stage shown in (5d) induces the large angle-of-attack. Nevertheless, the actual look angle does not violate the prescribed limit since the proposed law restricts the ideal look angle σ_M with the safety margin ε_σ as described above.

VI. Conclusion

In this study, we propose the look angle constrained impact angle control guidance law that only uses the bearing angles among the target information. To develop the guidance law, the surface variable that only consists of the line-of-sight angle and look angle is designed based on the kinematic conditions for achieving the impact angle constraint with confining the missile look angle within the pre-specified limit. The guidance law is derived to achieve the sliding mode of the defined surface variable. Since imposing the terminal impact angle constraint requires the curved trajectory, this capability to prevent the missile look angle from exceeding the prescribed limit is helpful from a practical standpoint. Furthermore, unlike the existing laws whose implementation demands the knowledge of the relative range or line-of-sight rate, the proposed guidance law only needs the line-of-sight angle and look angle among the target information. Hence, the proposed law can easily be implemented into a homing missile equipped with a structurally simple passive strapdown seeker. Both the theoretical analysis and the numerical simulation result indicate that the proposed guidance law achieves the desired tasks under bearings-only measurements.

Acknowledgments

This research is supported by the LIG Nex1 SNU and GNC Research Center (No. 0418-20170007)

References

[1] Kim, M. and Grider, K. V., "Terminal guidance for impact attitude angle constrained flight trajectories," *IEEE Transactions on Aerospace and Electronic Systems*, vol. 9, no. 6, pp. 852–859, 1973.

[2] Ryoo, C. K., Cho, H., and Tahk, M. J., "Optimal guidance laws with terminal impact angle constraint," *Journal of Guidance, Control, and Dynamics*, vol. 28, no. 4, pp. 724–732, 2005.

[3] ——, "Time-to-go weighted optimal guidance with impact angle constraints," *IEEE Transactions on Control Systems Technology*, vol. 14, no. 3, pp. 483–492, 2006.

[4] Kumar, S. R., Rao, S., and Ghose, D., "Sliding-mode guidance and control for all-aspect interceptors with terminal angle constraints," *Journal of Guidance, Control, and Dynamics*, vol. 35, no. 4, pp. 1230–1246, 2012.

[5] Lee, C.-H., Tahk, M.-J., and Lee, J.-I., "Generalized formulation of weighted optimal guidance laws with impact angle constraint," *IEEE Transactions on Aerospace and Electronic Systems*, vol. 49, no. 2, pp. 1317–1322, 2013.

[6] Kumar, S. R., Rao, S., and Ghose, D., "Nonsingular terminal sliding mode guidance with impact angle constraints," *Journal of Guidance, Control, and Dynamics*, vol. 37, no. 4, pp. 1114–1130, 2014.

[7] Bardhan, R. and Ghose, D., "Nonlinear differential games-based impact-angle-constrained guidance law," *Journal of Guidance, Control, and Dynamics*, vol. 38, no. 3, pp. 384–402, 2015.

[8] Cho, D., Kim, H. J., and Tahk, M.-j., "Impact angle constrained sliding mode guidance against maneuvering target with unknown acceleration," *IEEE Transactions on Aerospace and Electronic Systems*, vol. 51, no. 2, pp. 1310–1323, 2015.

[9] Hou, Z., Liu, L., Wang, Y., Huang, J., and Fan, H., "Terminal impact angle constraint guidance with dual sliding surfaces and model-free target acceleration estimator," *IEEE Transactions on Control Systems Technology*, vol. 25, no. 1, pp. 85–100, 2017.

[10] Ratnoo, A. and Ghose, D., "Impact angle constrained interception of stationary targets," *Journal of Guidance, Control, and Dynamics*, vol. 31, no. 6, pp. 1816–1821, 2008.

[11] ——, "Impact angle constrained guidance against nonstationary nonmaneuvering targets," *Journal of Guidance, Control, and Dynamics*, vol. 33, no. 1, pp. 269–275, 2010.

[12] Lee, C. H., Kim, T. H., Tahk, M. J., and Whang, I. H., "Polynomial guidance laws considering terminal impact angle and acceleration constraints," *IEEE Transactions on Aerospace and Electronic Systems*, vol. 49, no. 1, pp. 74–92, 2013.

[13] Kim, T.-H., Lee, C.-H., and Tahk, M.-J., "Time-to-go polynomial guidance with trajectory modulation for observability enhancement," *IEEE Transactions on Aerospace and Electronic Systems*, vol. 49, no. 1, pp. 55–73, 2013.

[14] Park, B.-G., Kim, T.-H., and Tahk, M.-J., "Optimal impact angle control guidance law considering the seeker's field-of-view limits," *Proceedings of the Institution of Mechanical Engineers, Part G: Journal of Aerospace Engineering*, vol. 227, no. 8, pp. 1347–1364, 2013.

[15] ——, "Range-to-go weighted optimal guidance with impact angle constraint and seeker's look angle limits," *IEEE Transactions on Aerospace and Electronic Systems*, vol. 52, no. 3, pp. 1241–1256, 2016.

[16] Erer, K. S. and Merttopcuoglu, O., "Indirect impact-angle-control against stationary targets using biased pure proportional navigation," *Journal of Guidance, Control, and Dynamics*, vol. 35, no. 2, pp. 700–704, 2012.

[17] Erer, K. S., Tekin, R., and Ozgoren, M. K., "Look angle constrained impact angle control based on proportional navigation," in *AIAA Guidance, Navigation, and Control Conference*, 2015, pp. 2015–0091.

[18] Tekin, R. and Erer, K. S., "Switched-gain guidance for impact angle control under physical constraints," *Journal of Guidance, Control, and Dynamics*, vol. 38, no. 2, pp. 205–216, 2015.

[19] Ratnoo, A., "Analysis of two-stage proportional navigation with heading constraints," *Journal of Guidance, Control, and Dynamics*, vol. 39, no. 1, pp. 156–164, 2016.

[20] Kim, T.-H., Park, B.-G., and Tahk, M.-J., "Bias-shaping method for biased proportional navigation with terminal-angle constraint," *Journal of Guidance, Control, and Dynamics*, vol. 36, no. 6, pp. 1810–1816, 2013.

[21] JASON, L. S. and ARTHUR, E., "Optimal programming problems with a bounded state space," *AIAA journal*, vol. 6, no. 8, 1968.

[22] Kim, H.-G. and Kim, H. J., "Impact time control guidance considering seeker's field-of-view limits," in *Decision and Control (CDC), 2016 IEEE 55th Conference on*. IEEE, 2016, pp. 4160–4165.

[23] ——, "Backstepping-based impact time control guidance law for missiles with reduced seeker field-of-view," *IEEE Transactions on Aerospace and Electronic Systems*, Accepted.

[24] Shtessel, Y., Edwards, C., Fridman, L., and Levant, A., *Sliding mode control and observation*. Springer, 2014.

[25] Cho, D., Kim, H. J., and Tahk, M.-J., "Nonsingular sliding mode guidance for impact time control," *Journal of Guidance, Control, and Dynamics*, 2015.

[26] Utkin, V., Guldner, J., and Shi, J., *Sliding mode control in electro-mechanical systems*. CRC press, 2009, vol. 34.

[27] Shima, T., Idan, M., and Golan, O. M., "Sliding-mode control for integrated missile autopilot guidance," *Journal of guidance, control, and dynamics*, vol. 29, no. 2, pp. 250–260, 2006.

Hyeong-Geun Kim received the B.S. and M.S. degrees in mechanical and aerospace engineering from Seoul National University, Seoul, Korea, in 2012 and 2014, respectively.

He is currently pursuing the Ph. D. degree in the Department of Mechanical and Aerospace Engineering at Seoul National University. His research interests include missile guidance and control, UAV autopilot design, and nonlinear control theory.

Jun-Yong Lee received the B.S. and M.S. degrees in mechanical engineering and aerospace engineering from Korea Advanced Institute of Science and Technology (KAIST) in 2014 and 2016, respectively.

He is currently pursuing the Ph. D. degree in the Department of Mechanical and Aerospace Engineering at Seoul National University. His research interests include missile guidance and control, autopilot design, and nonlinear control.

H. Jin Kim received the B.S. degree from Korea Advanced Institute of Science and Technology (KAIST) in 1995, and the M.S. and Ph.D. degrees in mechanical engineering from the University of California, Berkeley (UC Berkeley) in 1999 and 2001, respectively.

From 2002 to 2004, she was a Postdoctoral Researcher in Electrical Engineering and Computer Science, UC Berkeley. In September 2004, she joined the Department of Mechanical and Aerospace Engineering at Seoul National University, Seoul, Korea, as an Assistant Professor where she is currently at a Professor. Her research interests include intelligent control of robotic systems and motion planning.